Published in final edited form as:
FEBS Lett. 2012 April 5; 586(7): 1004–1008. doi:10.1016/j.febslet.2012.02.028.

Characterization of BshA, bacillithiol glycosyltransferase from *Staphylococcus aureus* and *Bacillus subtilis*

Heather Upton[1], **Gerald L. Newton**[2], **Melissa Gushiken**[1], **Kelly Lo**[2], **D. Holden**[1], **Robert C. Fahey**[2], and **Mamta Rawat**[1,*]

[1]Department of Biology, California State University-Fresno, Fresno, California, 93740

[2]Department of Chemistry and Biochemistry, The University of California at San Diego, La Jolla, California, 92093-0314

Abstract

The first step during bacillithiol (BSH) biosynthesis involves the formation of *N*-acetylglucosaminylmalate from UDP-*N*-acetylglucosamine and L-malate and is catalyzed by a GT4 class glycosyltransferase enzyme (BshA). Recombinant *Staphylococcus aureus* and *Bacillus subtilis* BshA were highly specific and active with L-malate but the former showed low activity with D-glyceric acid and the latter with D-malate. We show that BshA is inhibited by BSH and similarly that MshA (first enzyme of mycothiol biosynthesis) is inhibited by the final product MSH.

Keywords

mycothiol; bacillithiol; *Staphylococcus aureus*; glycosyltransferase; mycobacteria; thiol

Introduction

In nearly all eukaryotes, glutathione is the major low-molecular weight thiol that serves as a cofactor for a wide range of enzymes involved in protecting against reactive oxygen species, reactive nitrogen species, and many other toxins. GSH is found in most Gram-negative bacteria, including cyanobacteria, but only rarely in Gram-positive bacteria, which include a wide range of human pathogens. In the high GC Actinobacteria, a low-molecular-weight cysteine derivative called mycothiol (MSH) is the major thiol [1] while in the low GC Gram-positive bacteria, a similar thiol, bacillithiol (BSH), is present [2]. Both MSH and BSH contain the cysteinylglucosamine core moiety but in BSH L-malic acid is substituted for *myo*-inositol and the cysteine amino group is not acylated (Fig. 1a and 1b).

The first step in MSH biosynthesis involves the formation of *N*-acetylglucosaminylinositol-3- phosphate from UDP-*N*-acetyl glucosamine (UDP-GlcNAc) and 1-L-inositol-1-phosphate, a process catalyzed by a GT4 class glycosyltransferase (MshA) [3]. A similar first step occurs during BSH biosynthesis where a *B. subtilis* GT4

*To whom correspondence should be addressed. Dr. Mamta Rawat, Department of Biology, California State University-Fresno, Fresno, California 93740, USA, Fax: (559) 278-3963, Phone: (559) 278-2003, mrawat@csufresno.edu.

class glycosyltransferase enzyme (BshA) catalyzes the formation of *N*-acetylglucosaminylmalate (GlcNAc-Mal) from UDP-GlcNAc and L-malate (Fig. 1d) [4]. In 2008, Ruane et al. reported the crystal structure of a putative glycosyltransferase, ORF BA1558, which is the *B. anthracis* homolog of BshA [5]. Parsonage et al. (2010) reported the structure of this *B. anthracis* BshA with UDP-malate ternary complex and described the phenotype of the mutant disrupted in this gene [6]. Herein, we report on the characterization of *B. subtilis* BshA and *S. aureus* BshA and show that BSH is able to inhibit BshA. As a dominant thiol in significant pathogens, BSH biochemistry, in particular enzymes like BshA that are involved in the biosynthesis of BSH, may prove to be good targets for antibiotics directed against these pathogens.

Materials and Methods

Cloning and expression of *B. subtilis* and *S. aureus* BshA

BshA was PCR amplified from *B. subtilis* JH642 using primers BshAN5 (5'-CACCATGAGAAAACTAAA AATAGGA) and BshAN3 (5'-TCACTCCGGTTCTGCTAAATCGGC) and proofreading Pfu DNA polymerase (Stratagene) [7]. The amplicon was cloned into pet151 TOPO vector (Invitrogen) and expressed in BL-21 Star (DE3) pLysS *E. coli* strain as the N-terminal His-6 tagged protein. The protein was purified to homogeneity on a chelate chromatography nickel column (Clontech). The eluted proteins were dialyzed against the BshA assay buffer, 100 mM NaCl, 10 mM $MgCl_2$, and 25 mM HEPES pH 7.5, to which 1 mM β-mercaptoethanol was added and concentrated with Centricon 30 ultrafilter (Amicon) and snap frozen in 10% glycerol. Similarly, the *S. aureus* BshA was PCR amplified using SBshAN5 (5'-CACCATGAAGATAGGTATAAC) and SBshAN3 (5'- TTACTCGCCTTTACTTTTGTT), expressed and purified using PrepEase His tag protein purification Prep (USB Corporation). The BshA protein fraction was loaded onto a Sephadex G25 column to remove the imidazole and eluted with BshA assay buffer to which 2 mM dithiothreitol (DTT) was added. *S. aureus* BshA was snap frozen in individual aliquots in glycerol as it eluted off the column.

Assay for glycosyltransferase activity

S. aureus and *B. subtilis* BshA were assayed in 100 mM NaCl, 10 mM $MgCl_2$, and 25 mM HEPES pH 7.5 at 37°C with 2 mM DTT and 1 mM β-mercaptoethanol added to the buffer respectively. The consumption of UDP-GlcNAc and release of UDP were analyzed by HPLC with detection of peaks spectrophotometrically at 260 nm as previously described for MshA with minor modifications [3]. The following HPLC conditions were used: Buffer A: 2 mM tetrabutylammonium phosphate, pH 5.4; Buffer B: 20 mM KH_2PO_4, 50% methanol, 10 mM tetrabutylammonium phosphate, pH 5.4; elution program: 0-1 min, 15%B; 1 to 31 min, linear 15-100% Buffer B; 31-32 min, linear 100%-15% Buffer B; 45 min reinjection. The retention times for the standards, uridine, UMP, UDP-GlcNAc, UDP, and UTP were 4.9, 14.2, 20.5, 21.9, and 25.6 min, respectively. *S. aureus* BshA substrate specificity and *B. subtilis* BshA substrate specificity was determined.

Inhibition of BshA and MshA glycosyltransferase with BSH, MSH and O-UDP-GlcNAc

B. subtilis BshA was preincubated for 15 min at 37°C with various concentrations of BSH, diluted into the BshA reaction mixture, and glycosyltransferase activity was measured as the release of UDP as described above. The dose-response curves for BSH were determined in duplicate and half maximal inhibitory concentration (IC_{50}) calculated from these curves. Likewise, *M. smegmatis* cell lysate was preincubated with various concentrations of MSH, diluted into the MshA reaction mixture containing 1 mM 1-L-inositol-1-phosphate and 1 mM UDP-GlcNAc. To determine if 2',3'-dialdehydo-UDP-*N*-acetylglucosamine (O-UDP-

GlcNAc; Fig. 1c) from oxidation of UDP-GlcNAc inhibits BshA and/or MshA activity, both BshA and *M. smegmatis* cell lysate were preincubated with various concentrations of O-UDP-GlcNAc and activity assays performed.

Size determination of BshA glycosyl transferase

Gel filtration using Sephacryl 200 was used to determine the native molecular weight for both *S. aureus* and *B. subtilis* BshA. The following proteins were used to calibrate the column: cytochrome C, ovalbumin, bovine serum albumin, phophorylase B, aldehyde dehydrogenase, β amylase, and apoferritin.

Thiol determination

Briefly, 60 μg of purified protein was treated with 10 mM DTT, 10 mM diamide, or water at room temperature for 15 min. To denature the protein and stop the reaction, acetonitrile was added to the reaction followed by centrifugation to collect the pelleted protein. The pelleted protein was washed, brought up in 100 μl of 6 M guanidine HCl, and incubated at 37°C for 25 min. Protein concentration was determined by measuring absorbance at 280 nm. To measure the thiol content, the samples were treated with 0.16 mM 5,5'-dithiobis(2-nitrobenzoic acid) (DTNB) for 15 min and the absorbance at 412 nm was measured.

Molecular Modeling and Data analysis

To determine basic kinetic parameters for each substrate, initial velocity plots at saturating concentrations of one substrate were fit to the Michaelis-Menten equation. All data were analyzed using KaleidaGraph (Synergy Software).

Protein threading on *B. subtilis* and *S. aureus* BshA was performed using *B. anthracis* BA1558 X-Ray crystal structure (PDB accession no.: 2JJM) with IP, integer programming-based threading engine of RAPTOR [8] 3D structure modeling tool OWL and displayed with MolScript [9].

Results and Discussion

We recently identified the gene, *bshA*, responsible for the first step in the biosynthesis of BSH in *Bacillus subtilis* [4]. This gene codes for a retaining glycosyltransferase which uses L-malate as the acceptor substrate and UDP-GlcNAc as the donor substrate. Disruption of this gene in *B. subtilis* results in sensitivity to alkylating agents, fosfomycin and methylglyoxal, indicating involvement of BSH in detoxification of toxins, to environmental stresses such as osmotic stress and acid stress, protection against toxins and a decrease in sporulation [4].

In this report, we present a characterization of *B. subtilis* BshA and the medically relevant *S. aureus* BshA. When the two genes were expressed in *E. coli*, the resulting recombinant proteins behaved very differently during the purification process. *B. subtilis* BshA purification resulted in a good yield and the protein remained soluble even after concentration to 7mg ml^{-1}; however, *S. aureus* BshA started precipitating as the protein eluted off the Ni^{+} affinity column. Thus, we switched to commercially prepared Prep Ease His Tag Protein Purification columns for rapid purification of the protein followed by Sephadex G25 gel filtration column to rid eluent of imidazole. As the fractions were eluted, they were frozen in 10% glycerol to prevent further precipitation.

Both recombinant *S. aureus* and *B. subtilis* BshA exhibited marked activity when assayed by HPLC for UDP production using UDP-GlcNAc and L-malate as substrates. Both substrates exhibited Michaelis-Menten kinetics in the initial velocity plots for L-malate and UDP-

GlcNAc, and no curvature was seen in the Lineweaver-Burk linear replots (data not shown). The kinetic parameters for each substrate were determined after fitting to the Michaelis-Menten Equation. The apparent K_m for UDP-GlcNAc at 3 mM malate is within the significant error range (250 ± 110 μM for *S. aureus* and 370 ± 94 μM for *B. subtilis*) (Table 1). The apparent K_m for UDP-GlcNAc reported for *B. anthracis* BshA is equal to that of *B. subtilis* at 370 μM determined with the HPLC assay [6] and the apparent K_m for UDP-GlcNAc for *C. diptheraie* MshA is 210 ± 20 μM [10]. In contrast, the apparent K_m for L-malate is not within the significant error range between the *S. aureus* and *B. subtilis* enzymes (710 ± 110 μM for *S. aureus* BshA and 410 ± 70 μM for *B. subtilis* BshA) and the V_{max} for the *S. aureus* enzyme is also 3 to 4 fold higher than the *B. subtilis* enzyme. Substrate specificity studies further highlight the differences between the two enzymes with *S. aureus* BshA showing measurable specific activity with not only L-malate but D-glyceric acid and *B. subtilis* BshA showing measurable specific activity with L-malate and the entantiomer D-malate (Table 2). The k_{cat} calculated from the UDP-GlcNAc V_{max} is 24-25 sec^{-1} and 6.1-7.8 sec^{-1} for *S. aureus* and *B. subtilis* BshA, respectively. In comparison, the k_{cat} for *B. anthracis* BshA [6] and *Corynebacterium diptheraie* MshA [10] are 28 sec^{-1} and 12.5 sec^{-1} respectively.

In 2008, Ruane and colleagues [5] first reported the structure of *Bacillus anthracis* BshA (BA1558). Parsonage et al (2010) further crystallized this enzyme in complex with UDP and malate [6]. *B. anthracis* BshA has 63.1% sequence identity and 77.6% sequence similarity to *B. subtilis* BshA and 53.2% sequence identity and 72.5% sequence similarity to *S. aureus* BshA. We thus modeled the *S. aureus* and *B. subtilis* BshA on *B. anthracis* BshA. Molecular modeling indicated that all three proteins contain the typical GT-B fold of glycosyltransferases, which consists of two “Rossmann-like” beta/alpha/beta domains separated by a deep crevice in the inter-domain region and a kinked *C*-terminal α-helix that crosses over from the *C*-terminal domain to contact the *N*-terminal domain [5]. However there are some differences, most notably in the position of active site residues among the three proteins (Fig. 2). The active site Lys211 (Lys 212 in *B. subtilis* BshA, Lys 209 in *S. aureus* BshA), which binds to one of the phosphate oxygens of UDP, is present in an α-helix in approximately the same position in all three structures. On the other hand, the *B. anthracis* BshA His120 and *B. subtilis* BshA His121, which binds to malate, is present at the end of the β-sheet while *S. aureus* BshA His118 is in the middle of a β sheet. Also, the positions of the *B. anthracis* BshA Glu282 and Glu290 binding sites and the relevant amino acids in *B. subtilis* BshA (Glu283, Glu291) and *S. aureus* BshA (Glu280, Glu288) are very different among the three protein structures. Both residues are involved in substrate recognition of UDP, Glu282 binding to one of the phosphate oxygens of UDP and Glu290 binding to the ribose-2’-OH and ribose-3’-OH. These variations in the structure of the proteins may account for the difference in the behavior of the enzymes.

Ruane et al. (2008) [5] reported that *B. anthracis* monomers are arranged into a tetramer and Parsonage et al. (2010) [6] confirmed that *B. anthracis* BshA consists of eight monomers arranged as a dimer of tetramers. To determine if *B. subtilis* BshA and *S. aureus* BshA are also tetramers, gel filtration chromatography of purified recombinant proteins was conducted. *B. subtilis* BshA is composed of 377 amino acid residues with a monomer molecular weight of 42 kDa respectively. Analysis by gel filtration chromatography yielded apparent molecular weights of 160,000 kDa, suggesting that *B. subtilis* BshA is a tetramer. However, we were unable to determine the size of *S. aureus* BshA even after treatment with reducing agents, DTT and Tris(2-carboxyethyl) phosphine (TCEP) and alkylating agent, iodoacetamide, which resulted in precipitation of protein during gel filtration chromatography. To examine the oligomeric state of *S. aureus* BshA, thiol titration was performed in guanidine HCl using DTNB. In *S. aureus* BshA, three out of the four cysteines were free upon treatment with DTT and pretreatment with diamide, which oxidized the

cysteines, did not yield any free thiols. These results suggest that either one of the cysteine in the native protein is buried and inaccessible to DTT or is in the disulfide form. *S. aureus* BshA is thus also likely to form a disulfide linked dimer.

Regulation of BSH synthesis is likely to be multifactorial, including transcriptional control and feedback inhibition. GshA, γ-Glutamate-cysteine ligase, which catalyzes the first of two steps in the pathway for the biosynthesis of glutathione, is feedback-inhibited by glutathione [11] and CoA inhibits pantethonate kinase, the first enzyme in the CoA biosynthesis pathway [12]. To determine whether MSH and BSH biosynthesis are regulated by feedback inhibition, *B. subtilis* BshA and *M. smegmatis* cell lysate were pre-incubated with BSH and MSH respectively followed by the enzymatic assay. The IC_{50} for BSH inhibition of BshA is 0.7 mM, within the biological range for this thiol (Fig. 3), and the IC_{50} for MSH inhibition of MshA is 3.6 mM, also within the biological range for this thiol (Fig. 4a). Thus like glutathione and CoA, the levels of BSH of MSH are modulated by feedback inhibition of the first enzyme in the biosynthetic pathway.

BshA and MshA catalyze the first committed step in BSH and MSH biosynthesis respectively and thus these enzymes are considered to be potential drug targets. Recently, Frantom et al. (2011) reported that UDP-(5F)-GlcNAc, a sugar nucleotide with an electron withdrawing substituent, acts as a slow-binding, competitive inhibitor of *C. glutamicum* MshA (K_i ~1.6 μM) [13]. O-UDP-GlcNAc (Fig. 1c) inhibits UDP-*N*-acetylglucosamine 2-epimerase by binding to the UDP-GlcNAc binding site irreversibly [14]. As UDP-GlcNAc is a substrate for both BshA and MshA, O-UDP-GlcNAc was assayed for its ability to inhibit these enzymes. Preincubation of the inhibitor with the *M. smegmatis* cell lysate followed by the MshA assay resulted in an IC_{50} of 0.2 mM for MshA (Fig. 4b). Similar inhibition studies of BshA with O-UDP-GlcNAc did not show consistent inhibition. This inhibitor may serve as a basis for the chemical synthesis of further inhibitors for MshA.

Acknowledgments

This work was supported by NIH grants GM061223 to MR, AI072133 to RCF, and a MBRS RISE student stipend to HU.

References

1. Newton GL, Arnold K, Price MS, Sherrill C, delCardayre SB, Aharonowitz Y, Cohen G, Davies J, Fahey RC, Davis C. Distribution of thiols in microorganisms: mycothiol is a major thiol in most actinomycetes. J Bacteriol. 1996; 178:1990–1995. [PubMed: 8606174]
2. Newton GL, Rawat M, La Clair JJ, Jothivasan VK, Budiarto T, Hamilton CJ, Claiborne A, Helmann JD, Fahey RC. Bacillithiol is an antioxidant thiol produced in Bacilli. Nat Chem Biol. 2009; 5:625–627. [PubMed: 19578333]
3. Newton GL, Ta P, Bzymek KP, Fahey RC. Biochemistry of the initial steps of mycothiol biosynthesis. J Biol Chem. 2006; 281:33910–20. [PubMed: 16940050]
4. Gaballa A, Newton GL, Antelmann H, Parsonage D, Upton H, Rawat M, Claiborne A, Fahey RC, Helmann JD. Biosynthesis and functions of bacillithiol, a major low-molecular-weight thiol in Bacilli. Proc Natl Acad Sci USA. 2010; 107:6482–6. [PubMed: 20308541]
5. Ruane KM, Davies GJ, Martinez-Fleites C. Crystal structure of a family GT4 glycosyltransferase from *Bacillus anthracis* ORF BA1558. Proteins. 2008; 73:784–7. [PubMed: 18712829]
6. Parsonage D, Newton GL, Holder RC, Wallace BD, Paige C, Hamilton CJ, Dos Santos PC, Redinbo MR, Reid SD, Claiborne A. Characterization of the N-acetyl-α-D-glucosaminyl l-malate synthase and deacetylase functions for bacillithiol biosynthesis in *Bacillus anthracis*. Biochemistry. 2010; 49:8398–414. [PubMed: 20799687]
7. Sambrook, J.; Fritsch, EF.; Maniatis, T. Molecular cloning: a laboratory manual. 2. Cold Spring Harbor Laboratory Press; Plainview, NY: 1989.

8. Xu J, Li M, Kim D, Xu Y. RAPTOR: Optimal Protein Threading by Linear Programming. J Bioinform Comput Bio. 2003; 1:95–117. [PubMed: 15290783]
9. Kraulis PJ. MOLSCRIPT: a program to produce both detailed and schematic plots of protein structures. J Appl Cryst. 1991; 24:946–950.
10. Vetting MW, Frantom PA, Blanchard JS. Structural and enzymatic analysis of MshA from *Corynebacterium glutamicum*: substrate assisted catalysis. J Biol Chem. 2008; 283:15834–15844. [PubMed: 18390549]
11. Apontoweil P, Berends W. Glutathione biosynthesis in *Escherichia coli* K 12. Properties of the enzymes and regulation. Biochim Biophys Acta. 1975; 399:1–9. [PubMed: 238647]
12. Karasawa T, Yoshida K, Furukawa K, Hosoki K. Feedback Inhibition of Pantothenate Kinase by Coenzyme A and Possible Role of the Enzyme for the Regulation of Cellular Coenzyme A Level. J Biochem. 1972; 71:1065–1067. [PubMed: 5074271]
13. Frantom PA, Coward JK, Blanchard JS. UDP-(5F)-GlcNAc acts as a slow-binding inhibitor of MshA, a retaining glycosyltransferase. J Am Chem Soc. 2010; 132:6626–7. [PubMed: 20411981]
14. Blume A, Chen H, Reutter W, Schmidt RR, Hinderlich S. 2', 3'-Dialdehydo-UDP-N-acetylglucosamine inhibits UDP-N-acetylglucosamine 2-epimerase, the key enzyme of sialic acid biosynthesis. FEBS Lett. 2002; 521:127–32. [PubMed: 12067740]

Abbreviations

BSH	bacillithiol
MSH	mycothio
UDP-GlcNAc	UDP-*N*-acetyl glucosamine
GlcNAc-Mal	*N*-acetylglucosaminylmalate
DTT	dithiothreitol
DTNB	5,5'-dithiobis(2-nitrobenzoic acid)
TCEP	Tris(2-carboxyethyl) phosphine

Highlights

1. *Staphylococcus aureus* and *Bacillus subtilis* BshA, which catalyze the first step in bacillithiol biosynthesis, are highly specific and active with L-malate.
2. *S. aureus* BshA has low activity with D-glyceric acid while *B. subtilis* BshA has low activity with D-malic acid.
3. Feedback inhibition of BshA and MshA occurs with bacillithiol and mycothiol, respectively.

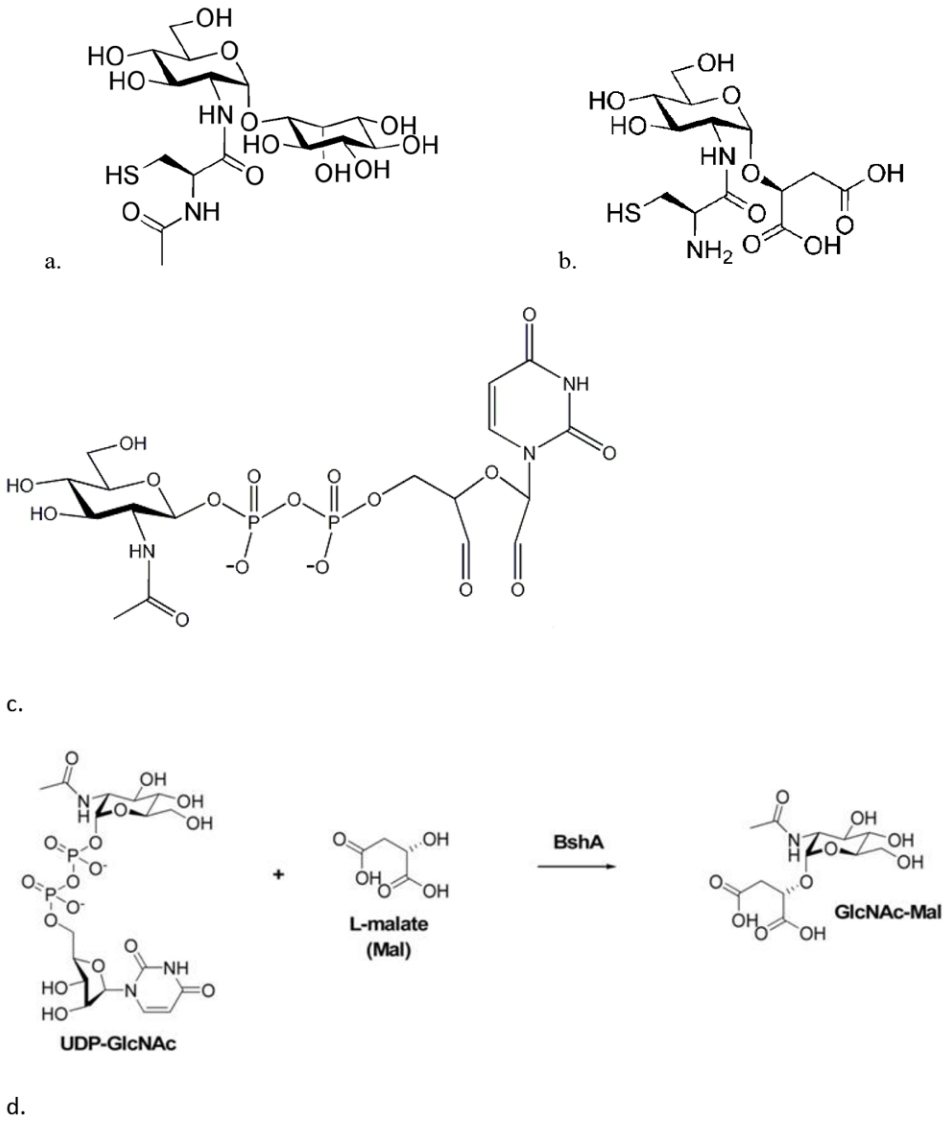

Fig. 1.

Structure of a) mycothiol, b) bacillithiol, c) O-UDP-N-acetylglucosamine (oxidized UDP-*N*-acetylglucosamine); note that the ribose moiety in UDP-*N*-acetylglucosamine has been oxidized to a dialdehydo- moiety, and d) BshA glycosyl transferase reaction

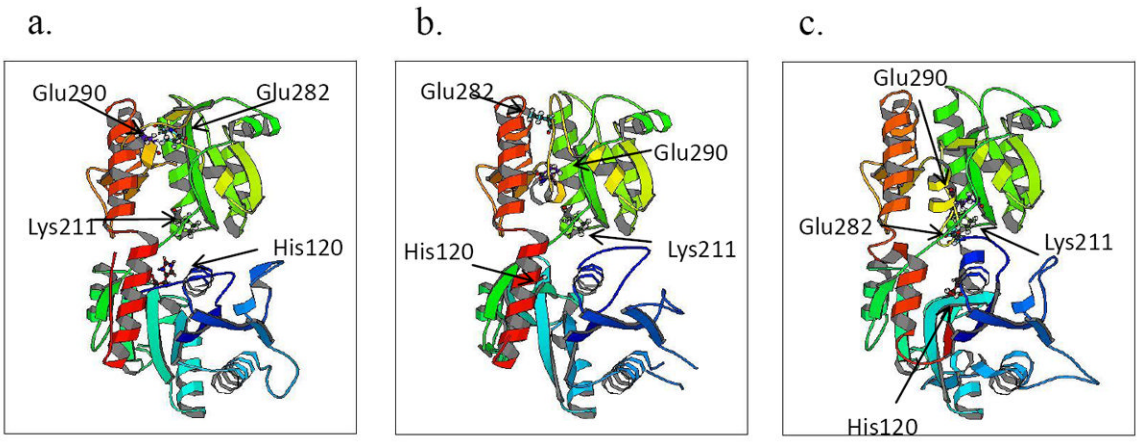

Fig. 2.

3D structure of *B. subtilis* and *S. aureus* BshA, a) *B. anthracis* BshA (BA1558), b) *B. subtilis* BshA, and c) *S. aureus* BshA. Residues identified in *S. aureus* and *B. subtilis* are equivalent to *B. anthracis* residue numbers.

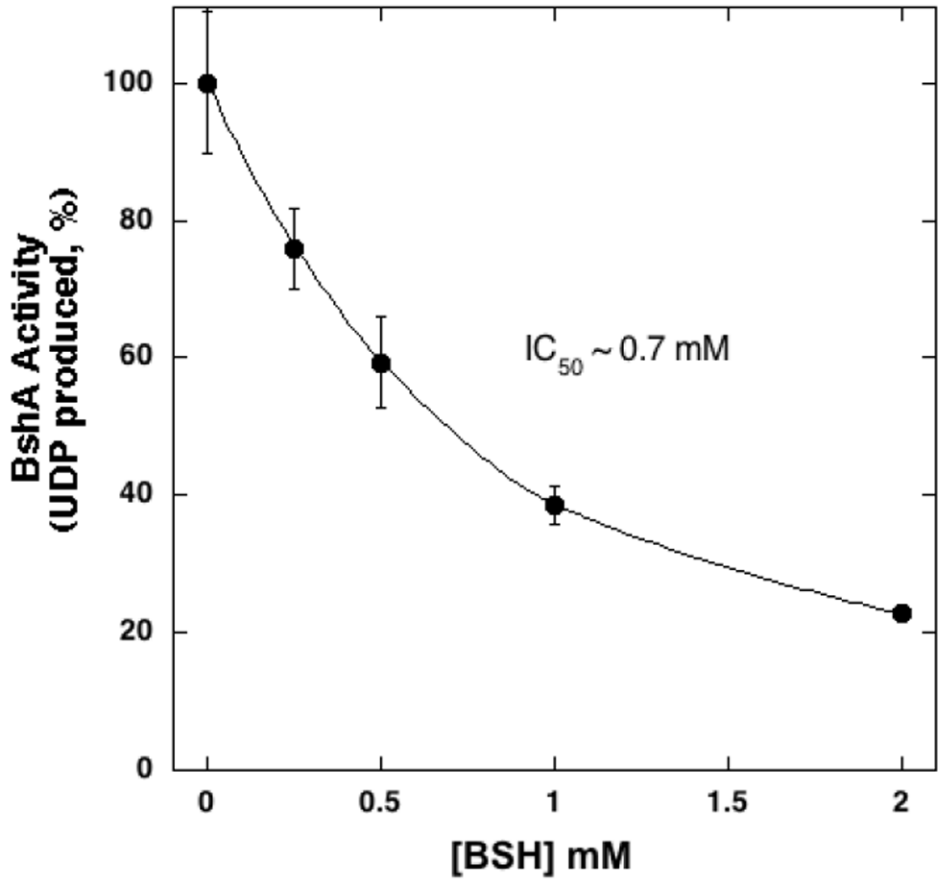

Fig. 3.

Inhibiton of *B. subtilis* BshA by BSH. a) *B. subtilis* BshA (0.71 μg) preincubated with BSH and assayed for BshA activity with 0.5mM UDP-GlcNAc and 0.5 mM L-malate

a.

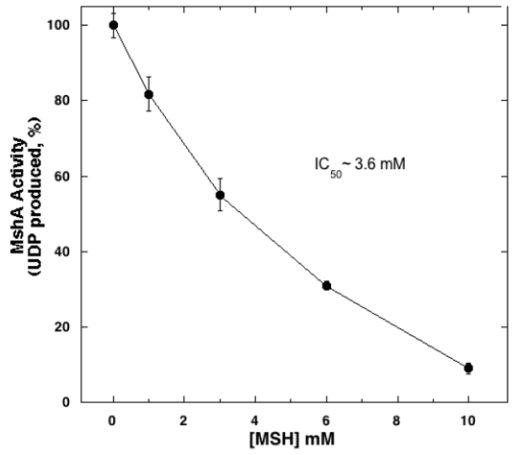

b.

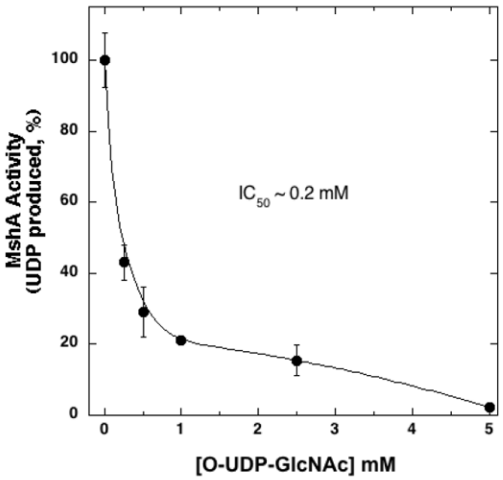

Fig. 4.

a) *M. smegmatis* cell free extract (2.7 mg total protein) preincubated with MSH and assayed for MshA activity with 1mM UDP-GlcNAc and 1mM 1-L-inositiol-1-phosphate. b) *M. smegmatis* cell free extract preincubated with O-UDP-GlcNAc and assayed for MshA activity with 1 mM UDP-GlcNAc and 1 mM 1-L-inositiol-1-phosphate. Control MshA rates, without inhibitor, were 0.4 nmoles min^{-1} mg $protein^{-1}$.

Table 1

Apparent K_m and V_{max} of *Staphylococcus aureus* and *Bacillus subtilis* BshA. For L-malate concentration dependence, 10 mM UDP-N-acetylglucosamine (UDP-GlcNAc) fixed and L-malate concentration varied from 0.1mM to 3.2 mM; for UDP-GlcNAc concentration dependence, 3 mM of L-malate fixed and UDP-GlcNAc varied from 1 mM to 15 mM; and, 0.35 μg BshA added to the reactions.

Substrate	K_m [μM]	V_{max} [nmol $min^{-1}mg^{-1}$]
L-malate		
S. aureus	710 ± 110	35 600 ± 1800
B. subtilis	410 ± 70	11 200 ± 100
UDP-GlcNAc		
S. aureus	250 ± 110	34 200 ± 3700
B. subtilis	370 ± 94	8700 ± 100

Table 2

Substrate specificity of *S. aureus* and *B. subtilis* BshA. For *B. subtilis* BshA, reaction conditions consisted of 0.3 mM acceptor substrate, 1.0 mM UDP-GlcNAc and 0.16 μg BshA. For *S. aureus* BshA, reaction conditions consisted of 0.7 mM acceptor substrate, 3.0 mM UDP-GlcNAc and 0.048 μg BshA.

	S. aureus		***B. subtilis***	
Substrate	**Specific Activity (nmoles min^{-1} mg^{-1})**	**Relative Rate (%)**	**Specific Activity (nmoles min^{-1} mg^{-1})**	**Relative Rate (%)**
L-malic acid	18,600 ± 6,300	100	6,600 ± 150	100
D-malic acid	<100	<0.5	230 ± 8	3.4
inositol-1-L-phosphate	<100	<0.5	<100	<0.5
glycolic acid	<100	<0.5	<100	<0.5
D-lactic acid	<100	<0.5	<100	<0.5
D, L-isocitric acid	<100	<0.5	<100	<0.5
D-glyceric acid	430 ± 180	2.3	<100	<0.5
citric acid	<100	<0.5	<100	<0.5